PROC. ITB Eng. Science Vol. 35 B, No. 2, 2003, 155-181

H_∞ Estimation Approach to Active Noise Control: Theory, Algorithm and Real-Time Implementation

Bambang Riyanto

Dept. Electrical Engineering, Institut Teknologi Bandung
Jalan Ganesha 10, Bandung, Indonesia
E-mail: briyanto@lskk.ee.itb.ac.id

Abstract. This paper presents an H_∞ estimation approach to active control of acoustic noise inside an enclosure. It is shown how H_∞ filter theory and algorithm can be effectively applied to active noise control to provide important robustness property. Real-time implementation of the algorithm is performed on Digital Signal Processor. Experimental comparison to conventional FxLMS algorithm for active noise control is presented for both single channel and multichannel cases. While providing some new results, this paper also serves as a brief review on H_∞ filter theory and on active noise control.

Keywords: *3D enclosure; active noise control; centralized; decentralized; digital signal processor; H_∞ filter algorithm; multichannel; single channel.*

1 Introduction

Acoustic noise can basically be described as unwanted sounds whose emergence can not be avoided. There are numerous sources of acoustic noise that we encounter everyday such as typical heavy daily traffic, airplanes passing above, fans, and air conditioners. Acoustic noise problems become more evident as more and more noisy equipment such as engines, transformers, and compressors are used in industry.

Traditional methods of attenuating acoustic noise involve the use of damping materials or sound absorbers. Such materials are placed around the noise source, or inside a room where noise is to be reduced. Other methods of noise reduction include using sound mufflers to protect the ears and moving the noise source to a remote location. The methods aforementioned are known as *passive* methods. Utilization of damping materials or sound absorbers are only effective for noise of high frequency. The reason for this is that the thickness of the material is proportional to the reciprocal of the frequency of noise. Thus for acoustic noise of low frequency one would need thicker materials, meaning adding more bulk (if we were to place dampers inside a vehicle such as a car, tractor or airplane) and providing more space for the materials. It is not a very economical choice either, as damping materials are quite expensive.

An alternative method to acoustic noise attenuation which has attracted a lot of attention recently is the *active* method of noise attenuation. Active noise control (which we shall abbreviate as ANC from this point on), as it is popularly known, is based on the principle of destructive interference between acoustic wave from a noise source and another acoustic wave from a different source (a secondary source, usually called the *anti-sound*). The control system generates a secondary signal which is 180^o out of phase with the noise signal and the superposition of the two signals will result in a minimum residual signal (the *residual noise*). The idea is illustrated in Figure 1.

Basically acoustic ANC is implemented using microphone(s) or any other type of sensor to convey some characteristic information on the acoustic noise source (called the *reference*) and detect the noise

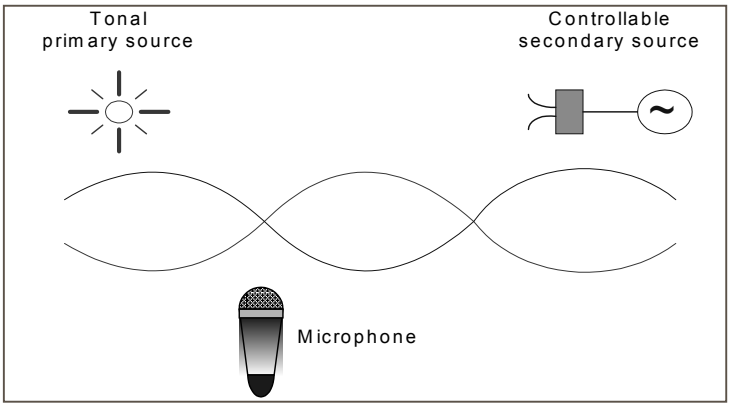

Figure 1 Principle of Active Noise Control.

signal (called the *error* signal) that is to be attenuated at a certain location(s) in space. To generate the secondary signals, or the *anti-sound*, actuators in the form of loudspeakers are generally employed. The idea has been around for a while and some analog ANC systems have been implemented. The problem with the analog system is that it was rather limited due to human intervention necessary in adjusting some necessary parameters [1,9]. In the early days of the development of adaptive signal processing, the impediment in applying the technique to active noise control was the sheer bulk of computation needed to achieve a system working in real time. Computing power demands in such an application were beyond the capability of microprocessors available at the time. Thanks to the recent advancement of digital signal processor (DSP), real-time implementation of ANC presently becomes feasible.

This paper presents investigation of adaptive H_∞ filter algorithm and its application to active control of acoustic noise inside a 3-D enclosure. Real-time implementation of the algorithm is performed on DSP. Experimental comparison to conventional FxLMS algorithm is presented for both single channel and multichannel cases. Specifically, contribution of this paper over existing literatures on active noise control [1,2,4,6,7,9,11,13-18] is twofold : 1) to investigate H_∞ filter performance in rejecting noise inside 3-D enclosure and its robustness property through real-time DSP based ANC experiment, 2) to extend its structure to multichannel case in both centralized and decentralized fashion. As an aside, this paper also studies how H_∞ filter is applied to ANC and should be modified by providing a state estimation interpretation of the feedforward ANC[3,5,8]. While providing some new results, this paper also serves as a brief review on H_∞ filter theory and on active noise control, although it is not aimed at providing exhaustive literature survey in these fields.

The rest of this paper is outlined as follows. In Section 2, single channel and multi-channel ANC are briefly discussed. In Section 3, feedforward ANC is presented. In Section 4, adaptive H_∞ filter for ANC is discussed. Experimental set-up and results are presented in Section 5. Finally, conclusion is drawn in Section 6.

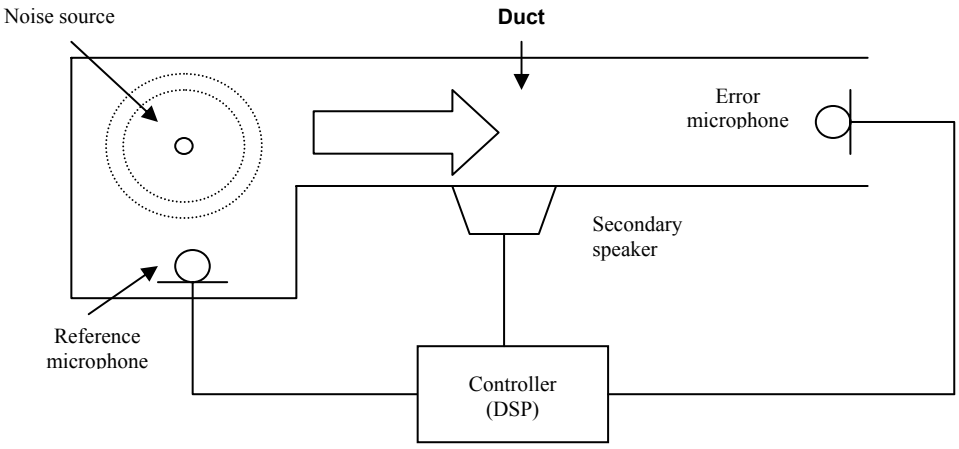

Figure 2 Single channel ANC inside a narrow duct.

2 Single Channel and Multi Channel ANC

Based on the number of error sensors and secondary actuators used in the system there are two types of ANC systems. If there is only one error sensor and a single secondary actuator then the system is called a single channel ANC.

It is typically used in situations where the acoustic wave can be assumed to be a plane wave traveling in one direction or if the waveform is not very complex such as in a narrow duct or pipe [1,6,9]. In such physical systems one actuator and one error sensor is sufficient to attenuate the noise encompassing a region encircling the sensor. Such a single channel ANC is illustrated in Figure 2 for active control of noise inside a duct.

When the noise to be controlled is in a relatively large volume of space such as in an enclosure or large dimension duct, the acoustic noise field is relatively more complex and we will be dealing with a standing wave rather than a simple planar wave [9]. The noise to be attenuated can be spread out in several different distant locations. Therefore to achieve widespread attenuation, a noise control system must be set up with multiple error sensors and multiple actuators, and perhaps multiple reference sensors too. Such a system is called the *multi-channel* ANC system and is commonly applied in 3-D enclosure. An example where multi-channel ANC could be implemented is in the cabin of a car or a commercial airplane. Figure 3 depicts the idea of a multi-channel ANC system.

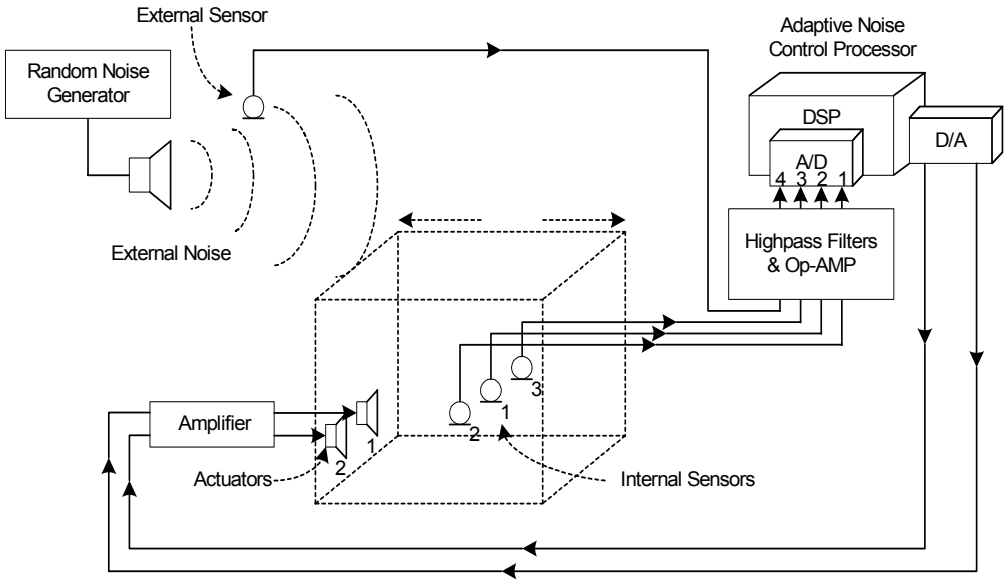

Figure 3 Multichannel ANC.

In real-life systems, characteristics of the acoustic noise source(s) and environment varies in time. The frequency, amplitude, phase and speed of sound is not really constant but is slowly changing (or statistically *non-stationary*). Thus the control system has to be adaptive and be able to track the

changes and tune its control signal accordingly. This is necessary so that the ANC system's stability and performance will be robust to such variations. In the multi-channel case this results in some compute-intensive algorithms [9,13] demanding powerful and fast digital signal processors for real-time implementation to be feasible.

Another fundamental problem to be considered in multi-channel ANC systems is determining what attenuation strategy we seek to carry out, i.e. the nature of the noise cancellation: global or local. Global attenuation is defined as reduction of the overall mean acoustic energy *throughout* the whole room or enclosure. Local attenuation refers to attenuation of noise in certain regions of the room or enclosure, usually surrounding the error microphones. Obviously, global attenuation is much more difficult to achieve and when the frequency content of the noise source is not low enough, a large number of microphones and secondary speakers will be needed [1,9] thus requiring more computing and is less practical to implement. On the other hand, local attenuation is more tractable. For example, in a car we may only require that noise be attenuated in the regions around a passengers head rather than throughout the whole cabin. Theoretically, the radius of the region surrounding the error microphone where the level of attenuation is still appreciable is approximately one-tenth the wavelength of the acoustic noise source. If the speed of sound is 340 m/s and the acoustic noise frequency is 100 Hz then this radius is about 34 cm but if the noise frequency is 1000 Hz then this radius drops to 3.4 cm. This is the reason why ANC will only be effective for attenuating low frequency noise. A disadvantage of the local attenuation strategy is that there is the possibility that the noise level of regions not surrounding the microphone may actually increase.

3 Adaptive Filters

As we have discussed in the first section, ANC systems must be adaptive as to be robust to variances in the statistical properties of the acoustic noise source(s) and environment. Some robust ANC systems have been implemented using analog controllers with fixed parameters [1,9] but the design is for a relatively stationary environment. Traditional approaches in adaptive ANC involving the use of linear adaptive filters as controllers (to produce the *control signals*) is motivated by the fact that propagation of sound wave is very linear at all but the highest of pressure levels (up to around 140 dB). Utilization of adaptive linear filters has been very successful and satisfying levels of acoustic noise cancellation have been obtained [1,2,4,6, 9]. In this section we will briefly discuss adaptive linear filters in the context of ANC but we will not get into a detailed mathematical analysis as this can be found in literatures such as [1,2,9,11,12].

One of the most popular algorithm in linear adaptive filtering is Widrow-Hoff's LMS algorithm [12]. This algorithm is very popular due to its sheer simplicity and ease of implementation. The adaptive linear filter in this case takes the form of a Finite Impulse Response (FIR) filter with adaptable weights. The diagram of the whole single input-single output (SISO) adaptive filter and all signals involved is depicted in Figure 4. The objective of the LMS algorithm is to minimize the Mean Square Error (MSE), $E[e(n)^2] = E[(d(n)-y(n))^2]$. Minimizing this quantity means that after the weights have stopped adapting (or more precisely have *converged*) the filter output $y(n)$ at time n will be close to the desired response $d(n)$.

The weights are adapted using a gradient descent algorithm, the weight vectors descending in the direction of $-\nabla_w E[e(n)^2]$. The gradient is approximated by $-\nabla_w e(n)^2$ because the quantity $E[e(n)^2]$ and $\nabla_w E[e(n)^2]$ can only be determined if we had an *ensemble* of identical filters and signals, which we do not have in practical cases. Thus in the LMS algorihm weight vector is adapted according to the recursive equation [9,12]:

$$w(n+1) = w(n) + 2\mu e(n)\mathbf{x}(n)$$

where the value μ is the adaptation rate which has a range of value $0<\mu<1$.

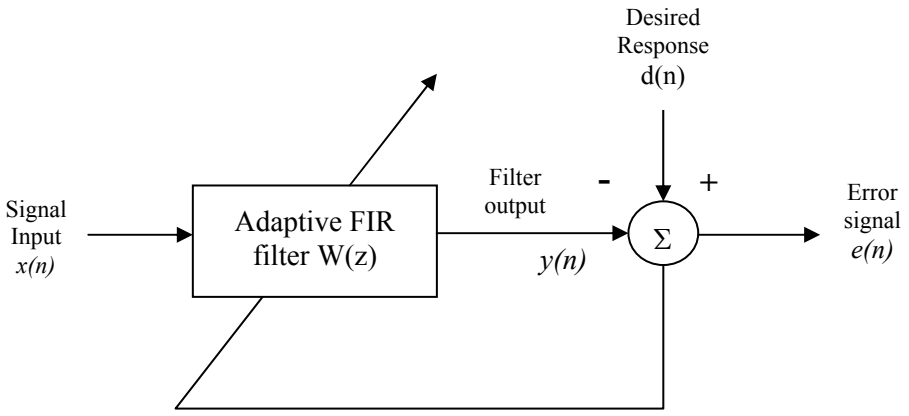

Figure 4 Structure of adaptive FIR filter and all signals involved.

The value of μ is very critical in the performance of the algorithm in terms of speed of convergence and steady state error and there are several criteria for finding a good value for μ [9]. To obtain better performance many variants of the LMS have been derived such as the Normalized LMS algoritm (NLMS), correlation LMS and others, see [9] for more details. Considering secondary

path effect, application of this algorithm to active noise control leads to FxLMS filter where the reference signal is filtered before applying it to LMS algorithm to produce antinoise signal.

4 H_∞ Filter Theory

In this section, H_∞ filter problems and their solutions are presented. Comparison to the classical Kalman filter will also be addressed. See [3,8,23] for more details. Dual control problems were addressed, for instance, in seminal work of [24], see also [19-22] for mixed H_2/H_∞ control problems. Much of the material of this section is summarized from [3].

Formulation of the H_∞-Filtering Problem
Suppose that a time-variant state-space model is given by

$$\begin{cases} x_{i+1} = F_i x_i + G_i u_i, \quad x_0 \\ y_i = H_i x_i + v_i, \quad i \geq 0 \end{cases} \tag{1}$$

where $F_i \in C^{nxn}$, $G_i \in C^{nxm}$ and $H_i \in C^{pxn}$ are known matrices, x_0, $\{u_i\}$, and $\{v_i\}$ are unknown quantities, and y_i is the measured output. In the state estimation problem, v_i can be viewed as a measurement noise and u_i as a process noise or driving disturbance. No assumption is made on the nature of the disturbances (e.g., normally distributed, uncorrelated, etc). Suppose that we would like to estimate some arbitrary linear combination of the states, say

$$z_i = L_i x_i$$

where $L_i \in C^{qxn}$ is given, using the observations $\{y_j\}$.

Now, denote $\breve{z}_{i|i} = F_f(y_0, y_1, \ldots, y_i)$ as the estimate of z_i given observations $\{y_j\}$ from time *0* to, and including, time *i,* and denote $\breve{z}_i = F_p(y_0, y_1, \ldots, y_{i-1})$ as the estimate of z_i given observation $\{y_j\}$ from time 0 to time *i–1*. The following two estimation errors can then be defined : the filtered error

$$e_{f,i} = \breve{z}_i\big|_i - L_i x_i \tag{2}$$

and the predicted error

$$e_{p,i} = \breve{z} - L_i x_i. \tag{3}$$

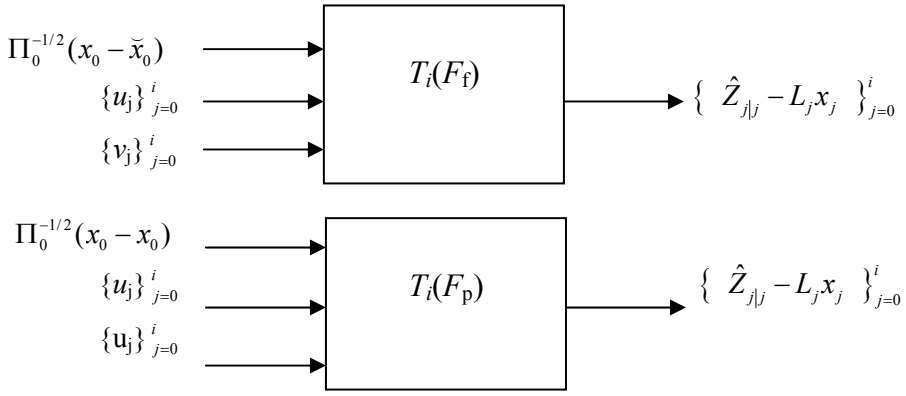

Figure 5 Transfer matrix from disturbances to filtered and predicted estimation errors.

Let $T_i(F_f)$ and $T_i(F_p)$ denote the transfer operators that map the unknown disturbances $\{\Pi_0^{-1/2}(x_0 - \breve{x}_0), \{u_j\}_{j=0}^{i}\}$ (where $\breve{x}_0$ denotes an initial guess for x_0, and Π_0 is a given positive definite matrix) to the filtered and predicted errors $\{e_{fj}\}_{j=0}^{i}$ and $\{e_{p,j}\}_{j=0}^{i}$, respectively, as shown in Figure 5. Next, define the H_∞ norm of a transfer operator T as

$$\|T\|_\infty = \sup_{u \in h_2, u \neq 0} \frac{\|Tu\|}{\|u\|_2}$$

where $\|u\|_2$ is the h_2-norm of the causal sequence $\{u_k\}$, i.e., $\|u\|_2^2 = \sum_{k=0}^{\infty} u_k^* u_k$. From the above equation, the H_∞ norm has the interpretation of being the maximum energy gain from the input u to the output y.

The Optimal H_∞ State Estimation Problem can now be formally stated as follows : Find H_∞-optimal estimation strategies $\breve{z}_{i|i} = F_f(y_0, y_1, ..., y_1)$ and $\breve{z}_i = F_p(y_0, y_1, ..., y_{i-1})$ that respectively minimize $\|T_i(F_f)\|_\infty$ and $\|T_i(F_p)\|_\infty$ and compute

$$\gamma_{f,o}^2 = \inf_{F_f} \|T_i(F_f\|_\infty^2$$

$$= \inf_{F_f} \sup_{x_0, u \in h_2, v \in h_2} \frac{\sum_{j=0}^{i} e^*_{f,j} e_{f,j}}{(x_0 - \breve{x}_0)^* \Pi_o^{-1} (x_0 - \breve{x}_0) + \sum_{j=0}^{i} u_j^* u_j + \sum_{j=0}^{i} v_j^* v_j} \tag{4}$$

and

$$\gamma_{p,o}^2 = \inf_{F_p} \left\| T_i(F_p) \right\|_\infty^2$$

$$= \inf_{F_p} \sup_{x_0, u \in h_2, v \in h_2} \frac{\sum_{j=0}^{i} e^*_{f,j} e_{f,j}}{(x_0 - \breve{x}_0)^* \Pi_o^{-1} (x_0 - \breve{x}_0) + \sum_{j=0}^{i} u_j^* u_j + \sum_{j=0}^{i-1} v_j^* v_j} \tag{5}$$

where Π_0 is a positive definite matrix that represents *a priori* knowledge as to how close initial state x_0 is to the initial guess $\breve{x}_{o.}$

A closer look at equation (5) reveals that the infimum is taken over all strictly causal estimators F_p, whereas in (4) the estimators F_f are only causal since they have additional access to y_i. Indeed, the solution to the H_∞ problem depends on the structure of the information available to the estimator. It is clear from the above problem formulation that H_∞ optimal estimators guarantee the smallest estimation error energy over all possible disturbances of fixed energy. Therefore, they provide robust behavior with respect to disturbance variation. Unfortunately, only in some particular cases, a closed form solution to the optimal H_∞ estimation problem is available. It is, therefore, common in practice to consider a relatively simpler subobtimal solution.

Sub-Optimal H_∞ Problem is formally be stated as follows : Given scalars $\gamma_f > 0$ and $\gamma_p > 0$, find H_∞ suboptimal estimation strategies $\breve{z}_{i|i} = F_f(y_0, y_1, ..., y_i)$ (known as an *a posteriori* filter) and $\breve{z}_i = F_p(y_0, y_1, ..., y_{i-1})$ (known as *a priori* filter) that respectively achieve $\left\| T_i(F_f) \right\|_\infty < \gamma_f$ and $\left\| T_i(F_p) \right\|_\infty < \gamma_p$. Stated equivalently, find estimation strategies that respectively satisfy

$$\sup_{x_0, u \in h_2, v \in h_2} \frac{\sum_{j=0}^{i} e^*_{f,j} e_{f,j}}{(x_0 - \breve{x}_0) * \Pi_0^{-1} (x_0 - \breve{x}_0) + \sum_{j=0}^{i} u_j^* u_j + \sum_{j=0}^{i} v_j^* v_j} < \gamma_f^2 \tag{6}$$

and

$$\sup_{x_0, u \in h_2, v \in h_2} \frac{\sum_{j=0}^{i} e^*_{p,j} e_{p,j}}{(x_o - \breve{x}_0)^* \Pi_0^{-1} (x_o - \breve{x}_0) + \sum_{j=0}^{i-1} u_j^* u_j + \sum_{j=0}^{i-1} v_j^* v_j} < \gamma_p^2 \tag{7}$$

Obviously, it requires checking whether $\gamma_f \geq \gamma_{f,o}$ and $\gamma_p \geq \gamma_{p,o.}$

Solutions to Optimal H_∞ State Estimation Problem can be obtained to desired accuracy by iterating on the γ_f and γ_p of Sub-Optimal H_∞ Problem. Due to its simplicity, we shall be only dealing with suboptimal problem.

Note that the problems defined above are finite-horizon problems. So-called infinite-horizon problems can be considered if we define $T(F_f)$ and $T(F_p)$ as the transfer operators that map $\left\{x_0-\breve{x}_0,\left\{u_j\right\}_{j=0}^{\infty},\left\{v_j\right\}_{j=0}^{\infty}\right\}$ to $\left\{e_{f,j}\right\}_{j=0}^{\infty}$ and $\left\{e_{p,j}\right\}_{j=0,}^{\infty}$ respectively. Then by guaranteeing $\left\|T_i(F_f)\right\|_{\infty}<\gamma_f$ and $\left\|T_i(F_p)\right\|_{\infty}<\gamma_p$ for all i, we can solve the infinite horizon problems $\left\|T(F_f)\right\|_{\infty}\le\gamma_f$ and $\left\|T(F_p)\right\|_{\infty}\le y_{p,}$ respectively. Direct solutions, however, are also possible.

Solution of the suboptimal H^{∞} Filtering Problem

The existing solutions (see, e.g., [8], [23]) to the suboptimal H_{∞} filtering problem can now be presented. As we shall see, they are intriguingly similar in several ways to the conventional Kalman filter. It was this similarity in structure that led authors of [3] to extend Kalman filters in Krein space.

Theorem 1 (An H_{∞} *A Posteriori Filter*)[3, 8, 23]: For a given $\gamma>0$, if the $[F_j \quad G_j]$ have full rank, then an estimator that achieves $\left\| T_i (F_f) \right\|_{\infty}<\gamma$ exists if, and only if

$$P_j^{-1}+H_j^*H_j-\gamma^{-2}L_j^*L_j>0, \quad j=0,...,i \tag{8}$$

where $P_0=\Pi_0$ and P_j satisfies the Riccati recursion

$$P_j+i=F_jF_jF_j^*+G_jG_j^*-F_jP_j[H_j^* \quad L_j^*]R_{e,j}^{-1}\begin{bmatrix}H_j\\L_j\end{bmatrix}P_jF_j^* \tag{9}$$

with

$$R_{e,j}=\begin{bmatrix}I & 0\\0 & -\gamma^2 I\end{bmatrix}+\begin{bmatrix}H_j\\L_j\end{bmatrix}P_j[H_j^* \quad L_j^*]. \tag{10}$$

If this is the case, then one possible level -γ H_{∞} filter is given by

$$\breve{z}_j\Big|_j=L_j\hat{x}_j\Big|_j$$

where $\hat{x}_j\Big|_j$ is recursively computed as

$$\begin{aligned}&\hat{x}_j+1\Big|j+1=F_j\,\hat{x}_j\Big|+K_{s,j+1}(y_j+1-H_{j+1}F_j\hat{x}_j\Big|_j)\\&\hat{x}-1\Big|-1=\text{ initial guess}\end{aligned} \tag{11}$$

and

$$K_{s,j+1}=P_{j+1}H_{j+1}^*(I+H_{j+1}P_{j+1}H_{j+1}^*)^{-1}. \tag{12}$$

Theorem 2 (*An H^∞ A Priori Filter*) [3,8,23]: For a given $\gamma > 0$, if the $[F_f \;\; G_j]$ have full rank, then an estimator that achieves $\| T_i(F_p) \|_\infty < \gamma$ exists if, and only if

$$\tilde{p}_j^{-1} = P_j^{-1} - \gamma^{-2} L_j^* L_j > 0, \quad j = 0,...,i \tag{13}$$

where P_j is the same as in Theorem 1. If this is the case, then one possible level -γ H_∞ filter is given by

$$\breve{z}_j = L_j \hat{x}_j \tag{14}$$

$$\hat{x}_{j+1} = F_j \hat{x}_j + K_{a,j}(y_j - H_j \hat{x}_j)$$

$$\hat{x}_0 = \text{ initial guess} \tag{15}$$

where

$$K_{a,j} = F_j \tilde{P}_j H_j^* (I + H_j \tilde{P}_j H_j^*)^{-1} \tag{16}$$

Comparisons with the Kalman Filter

As is well known, the Kalman-filter algorithm for estimating the states in (1), assuming that the $\{u_i\}$ and $\{v_i\}$ are now uncorrelated unit variance white noise processes, is

$$\hat{x}_{j+1} = F_j \hat{x}_j + F_j P_j H_j^* (I + H_j P_j H_j^*)^{-1} (y_j - H_j \hat{x}_j)$$

$$\hat{x}_{j+1|j+1} = F_j \hat{x}_{j|j} + P_{j+1} H_{j+1}^* (I + H_{j+1} P_{j+1} H_{j+1}^*)^{-1} (y_{j+1} - H_{j+1} \hat{x}_{j+1})$$

where

$$P_{j+1} = F_j P_j F_j^* + G_j G_j^* - F_j P_j (I + H_j P_j H_j^*)^{-1} P_j F_j^*, \quad P_0 = \Pi_0.$$

As pointed out by several authors[3,8,23], the H_∞ solutions are very similar to the conventional Kalman filter. The major differences are the following:

- As can be seen from Riccati recursion (9), the structure of the H_∞ estimators depends on the linear combination of the states that we intend to estimate (i.e., the L_i). In contrast, in case of the Kalman filter, the estimate of any linear combination of the state is given by that linear combination of the state estimate. Intuitively, this means that the H_∞ filters are specifically tuned toward the linear combination $L_i x_i$.
- Additional conditions, (8) or (13), must be satisfied for the H_∞ filter to exist; in the Kalman filter problem the L_i would not appear, and the P_i would be positive definite so that (8) and (13) would be automatically satisfied.

- Indefinite (covariance) matrices, e.g., $\begin{bmatrix} I & o \\ o & -\gamma^2 I \end{bmatrix}$ appears versus just I in the Kalman filter.
- As $\gamma \to \infty$, the Riccati recursion (9) reduces to the Kalman filter recursion (17). This indicates that the H^∞ norm of the conventional kalman filter may be quite large, and that it may have poor robustness properties. Note also that condition (13) is more stringent than condition (8), showing that the existence of an *a priori* filter of level γ implies the existence of an *a posteriori* filter of level γ, but not necessarily vice versa.)

Although there are differences between H_∞ solutions and Kalman filter, it has been shown in [3] that the filters of Theorems 1 and 2 can in fact be obtained as certain Kalman filters, not in an H^2 (Hilbert) spaces, but in a certain indefinite vector space called a Krein space. The indefinite covariance and the appearance of L_i in the Riccati equation was explained easily in this framework. The additional condition (8) arises from the fact that in Krein space, unlike as in the usual Hilbert space context, quadratic forms need not always have minima or maxima unless certain additional conditions are met [3].

Parameterization of all H_∞ A Posteriori Filters
The filter of Theorem 1 is one among many possible filters with attenuation level γ. Explicit characterization of all possible estimators is given in the following theorem.

Theorem 3 (*All H_∞ A Posteriori Estimators*)[3]; All H_∞ *a posteriori* estimators that achieve a level γ_f (assuming they exist) are given by

$$\breve{z}_{j|j} = L_j \hat{x}_{j|j} + [\gamma_f^2 I - L_j (P_j^{-1} + H_j^* H_j)^{-1} L_j^*]^{\frac{1}{2}}$$
$$\times S_j((I + H_j P_j H_j^*)^{\frac{1}{2}}(y_j - H_j \hat{x}_{j|j}),\ldots,\ (I + H_0 P_0 H_0^*)^{\frac{1}{2}}(y_j - H_0 \hat{x}_{0|0})) \tag{17}$$

where $\hat{x}_{j|j}$ satisfies the recursion

$$\hat{x}_{j+1|j+1} = F_j \hat{x}_{j|j} + K_{s,j+1}(y_{j+1} - H_{j+1} F_j \hat{x}_{j|j}) - K_{c,j}(\breve{z}_{j|j} - L_j \hat{x}_{j|j}) \tag{18}$$

with $K_{s,j+1}$ the same as in theorem 1

$$K_{c,j} = (I + P_{j+1} H_{j+1} H_{j+1}^*)^{-1} F_j (P_j^{-1} + H_j H_j^* - \gamma_f^{-2} L_j L_j^*)^{-1} L_j^* \tag{19}$$

and

$$S(a_j,...,a_0)=\begin{bmatrix} S_0(a_0) \\ S_1(a_1,a_0) \\ \vdots \\ S_j(a_j,...,a_0) \end{bmatrix}$$

is any (possibly nonlinear) contractive causal mapping, i.e.,

$$\sum_{j=0}^{k}\left|S_j(a_j,...,a_0)\right|^2 < \sum_{j=0}^{k}\left|a_j\right|^2 \quad \text{for all } k = 0,1,\ldots,i.$$

Note that when the contraction of Theorem 3 is chosen as *S=0*, then we have $\breve{z}_{j|j} = L_j\hat{x}_{j|j,}$ and (18) reduces to the recursion of Theorem 1. Furthermore, the full parameterization of all H_∞ filters with level γ_f is given by a nonlinear causal contractive mapping *S*, despite the fact that the filter obtained in Theorem 1 is linear . The filter of Theorem 1 is known as the central filter, and as we have seen, corresponds to *S = 0*. This central filter has a number of other interesting properties. It corresponds to the risk-sensitive optimal filter and can be shown to be the maximum entropy filter. Moreover, in the game theoretic formulation of the H_∞ problem, the central filter corresponds to the solution of the game.

All H^∞ A Priori Filters

Full parameterization of all H_∞ apriori estimators is given in the following theorem.

Theorem 4 (*All H_∞ A Priori Estimators*)[3]: All H_∞ a priori estimators that achieves a level γ_p (assuming they exist) are given by

$$\hat{z}_j = L_j\hat{x}_j + (\gamma_p^2 I - L_j P L_j^*)^{\frac{1}{2}}\ S_j((I + H_{j-1}P_{j-1}H_{j-1}^*)^{-\frac{1}{2}}(y_{j-1} - H_{j-1}\overline{x}_{j-1}),\ldots,$$

$$\times(I + H_0\tilde{P}H_0^{*-\frac{1}{2}}(y_0 - H_0\overline{x}_0)) \tag{20}$$

where

$$\overline{x}_k = \hat{x}_k + P_k L_k^*(-\gamma_p^2 I + L_k L_k^*)^{-1}(\breve{z}_k - L\hat{x}_k) \tag{21}$$

$\hat{x}_j$ satisfies the recursion

$$\hat{x}_{j+1|j} = F_j\hat{x}_{j|j-1} + F_j P_j[L_j^* \quad H_j^*] \times R_{e,j}^{-1}\begin{bmatrix} \breve{z}_j - L_j\hat{x}_{j|j-1} \\ y_j - H_j\hat{x}_{j|j-1} \end{bmatrix} \tag{22}$$

with $P_j, \overline{P}_j$, and $R_{e,j}$ given by Theorem 2 and S is any (possibly nonlinear) contractive causal mapping.

5 H_∞ Estimation Interpretation of Active Noise Control

The objective of noise cancellation is to generate control signal $u(k)$, such that secondary output signal $y(k)$ is, in some sense, sufficiently close to primary signal $d(k)$ by using available measurement, as shown in Figure 6.

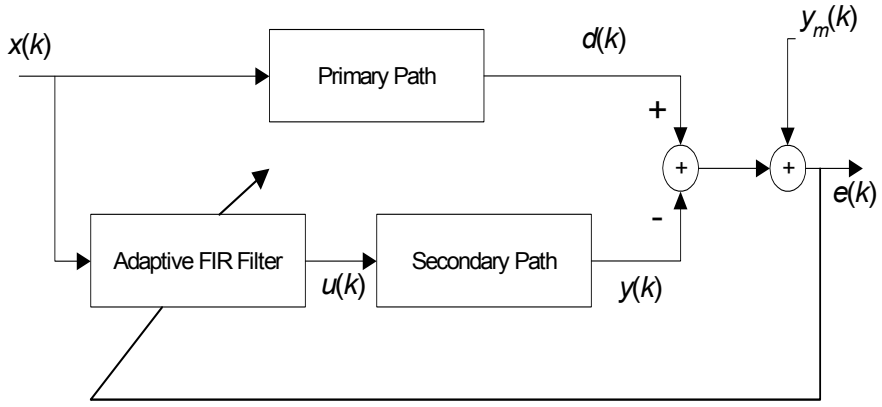

Figure 6 Block diagram of feedforward ANC.

The feedforward ANC can also be viewed as the problem of producing $y(k)$ as an estimation of $d(k)$, where, $x(k)$ is reference signal (primary noise), $y(k)$ is the secondary output, $e(k)$ is noise residue which is utilized to adjust adaptive filter, $v_m(k)$ is the external disturbance which models measurement noise, uncertainties in initial conditions, and modeling error[5,10]. The reference signal is applied to adaptive FIR filter through reference microphone, while noise residue is the actual signal measured by error microphone. Output of FIR filter, $u(k)$, is applied to secondary path through a speaker, which in turn generates antinoise signal. Note that, FIR filter cascaded with secondary path is an approximated model of unknown primary path. In Figure 7, the feedforward active noise cancellation is redrawn where primary path is replaced with approximated model. The approximated model is constructed from the knowledge of FIR filter and the secondary path. Note that as long as the modeling error is bounded, it can be viewed as disturbance signal component, $v_m(k)$.

As shown in Figure 7, $e(k) = d(k) - y(k) + v_m(k)$, where $e(k)$ signal measured by error microphone. The measurement component in the estimation process presented in the subsequent discussion is given by

$$m(k) \equiv e(k) + y(k) = d(k) + v_m(k) \tag{23}$$

Assume that $[A_s(k), B_s(k), C_s(k), D_s(k)]$ is state space representation of the copy of secondary path. Denote $W(k) = [w_0(k), w_1(k), ...,w_N(k)]^T$ and $\theta(k)^T$ as dynamic state vector of FIR and of secondary path dynamic, respectively. Using $\xi_k^T = [W(k)^T\ \theta(k)^T]$, the augmented system is given by

$$\overbrace{\begin{bmatrix} W(k+1) \\ \theta(k+1) \end{bmatrix}}^{\xi_{k+1}} = \overbrace{\begin{bmatrix} I_{(N+1)x(N+1)} & 0 \\ B_s(k)h_k^* & A_s(k) \end{bmatrix}}^{F_k} \overbrace{\begin{bmatrix} W(k) \\ \theta(k) \end{bmatrix}}^{\xi_k} \tag{24}$$

where $h_k = [x(k)\ x(k\text{-}1)\ \ldots\ x(k\text{-}N)]$ covers the effect of reference signal $x(.)$. Measured output is modeled as

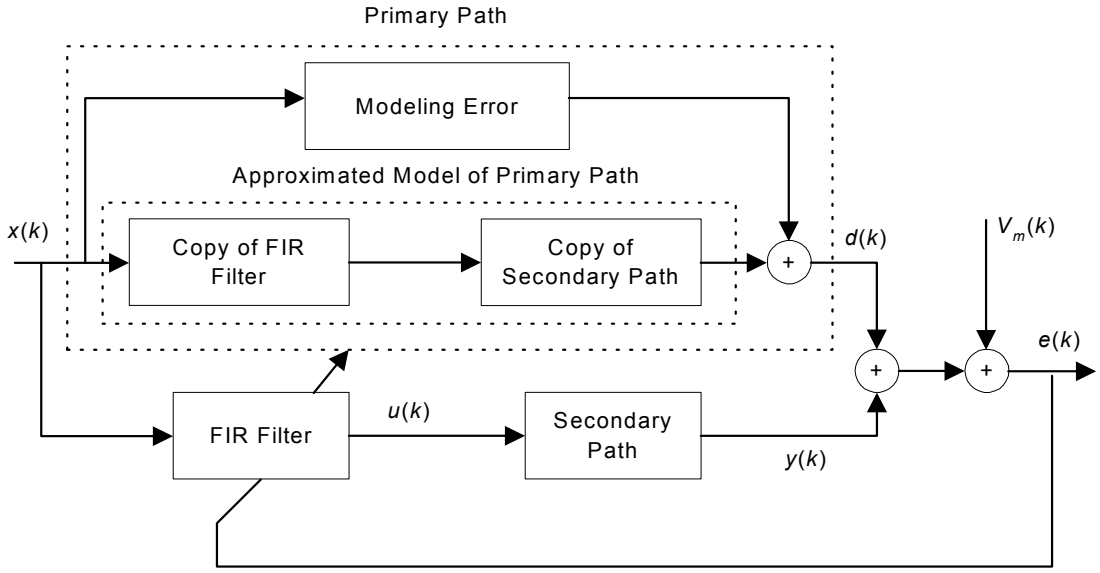

Figure 7 Model approximation of primary path.

$$m(k) = \overbrace{\begin{bmatrix} D_s(k)h_k^* & C_s(k) \end{bmatrix}}^{H_k} \begin{bmatrix} W(k) \\ \theta(k) \end{bmatrix} \tag{25}$$

with $m(k)$ as defined in (23). Now, assume that linear combination of state be defined as the estimated variable

$$s(k) = [\overbrace{L_{1,k}}^{L_k} \; L_{2,k}] \begin{bmatrix} w(k) \\ \theta(k) \end{bmatrix} \tag{26}$$

where $m(.) \in R^{p\text{x}1}$, $s(.) \in R^{q\text{x}1}$, $\theta(.) \in R^{r\text{x}1}$ and $W(.) \in R^{(N+1)\text{x}1}$. Furthermore, one can choose $L_k = H_k$. The estimation problem is shown in Figure 8, comprising two major parts : FIR Filter and Secondary Path Model.

Our objective in the active noise cancellation is to constrain worst-case of energy gain of estimated error s(k) under the presence of measurement disturbance and uncertainties in initial conditions. In other words, we seek sub-optimal H_∞ causal estimator $\hat{s}(k|k) = F(m(0),...,m(k))$ which satisfies

$$\sup_{v_m, \xi_0} \frac{\sum_{k=0}^{M} [s(k) - \hat{s}(k|k)]^* [s(k) - \hat{s}(k|k)]}{\xi_0^* \Pi_0^{-1} \xi_0 + \sum_{k=0}^{M} V_m^*(k) v_m(k)} \le \gamma^2 \tag{27}$$

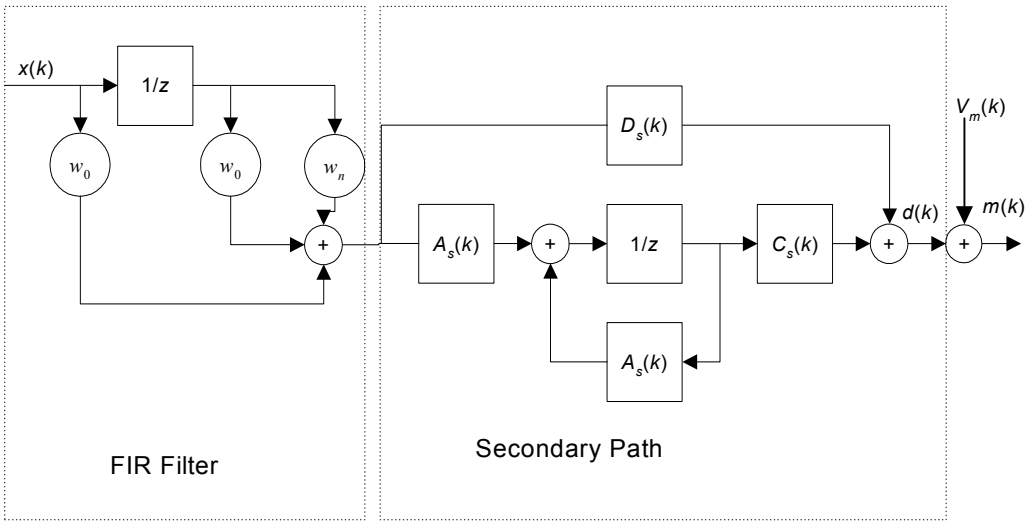

Figure 8 Estimation problem.

for a prespecified $\gamma > 0$. As shown previously, solution to the Finite Horizon γ-Suboptimal Filter is given as follows : There exists a positive value γ satisfying (27), if and only if, matrices R_k and $R_{e,k}$ defined by

$$R_{e,k} = \overbrace{\begin{bmatrix} I_p & 0 \\ 0 & -\gamma^2 I_q \end{bmatrix}}^{R_k} + \begin{bmatrix} H_k \\ L_k \end{bmatrix} P_k [H_k^* \quad L_k^*] \tag{28}$$

have the same inertia for all $0 \le k \le M$, where $P_0 = \Pi_{0 \text{ and}} P_k > 0$ satisfies recursive Riccati equation,

$$P_{k+1} = F_k P_k F_k^* - K_{p,k} R_{e,k} K_{p,k}^* \tag{29}$$

with $K_{p,k} = (F_k P_k [H_k^* \; L_k^*])$. In this case the H_∞ central estimator is given by

$$\hat{\xi}_{k+1} = F_k \hat{\xi}_k + K_{1,k}(m(k) - H_k \hat{\xi}_k), \qquad \hat{\xi}_0 = 0 \tag{30}$$

$$\hat{S}(k/k) = L_k \hat{\xi} + (L_k P_k H_k^*) R_{He,k}^{-1} (m(k) - \hat{H}_k \hat{\xi}_k) \tag{31}$$

where $K_{1,k} = (F_k P_k H_k^*) R_{He,k}^*$ and $R_{He,k} = I_P + H_k P_k H_k^*$.

Based on this result, the adaptive filter algorithm which provides robustness guarantee proceeds as follows[5,10] :

1. Set $\hat{W}(0) = \hat{W}_0$, $\hat{\theta}(0) = \hat{\theta}_0$ as an estimator of initial values for state vector of primary path approximation. Assume that $\theta_{\text{actual}}(0) = \theta_{actual,0}$, and that $\theta_{copy}(0) = \theta_{copy,0}$. Denoting $d(0)$ as primary path output, then for $0 \le k \le M$ (*finite horizon*):
2. Calculate control signal $u(k) = h_k^* \hat{W}(k)$,
3. Using the control signal for secondary path, the dynamics of actual state vector and output is given by

$$\theta_{\text{actual}}(k+1) = A_s(k)\theta_{\text{actual}}(k) + B_s(k)u(k)$$
$$y(k) = C_s(k)\theta_{\text{actual}}(k) + D_s(k)u(k) \tag{32}$$

4. Propagate *internal copy* of secondary state vector and output through

$$\theta_{copy}(k+1) = A_s(k)\theta_{copy}(k) + B_s(k)u(k)$$
$$y(k) = C_s(k)\theta_{copy}(k) + D_s(k)u(k)$$

5. Calculate measurement vector, $m(k)$, through direct measurement $e(k)$, according to $m(k) = e(k) + y_{copy}(k)$,
6. Use the state updating in Equation (32)
7. If $k \le M$ go to Step 2

Diagram block of the adaptive H_∞ filter algorithm is shown in Figure 9.

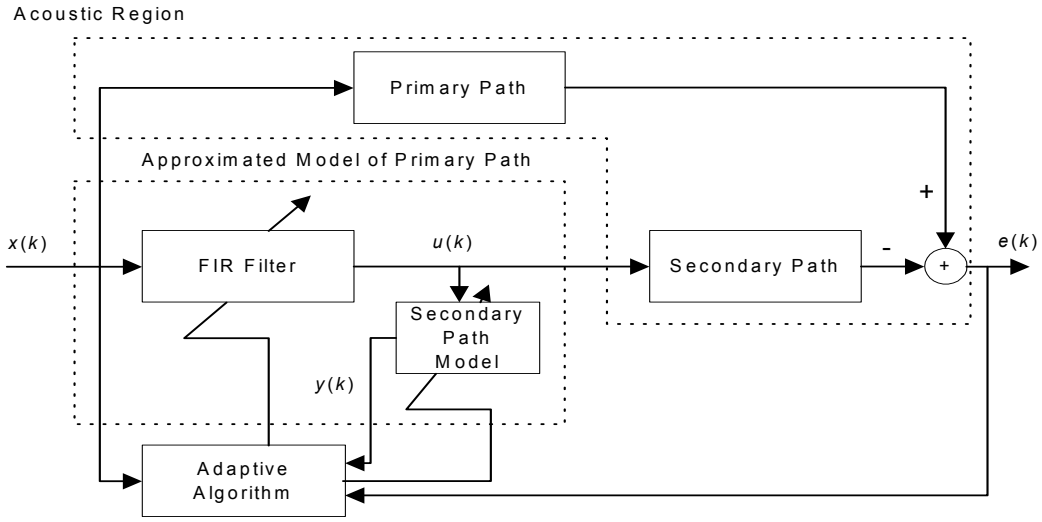

Figure 9 Adaptive H_∞ filter in ANC.

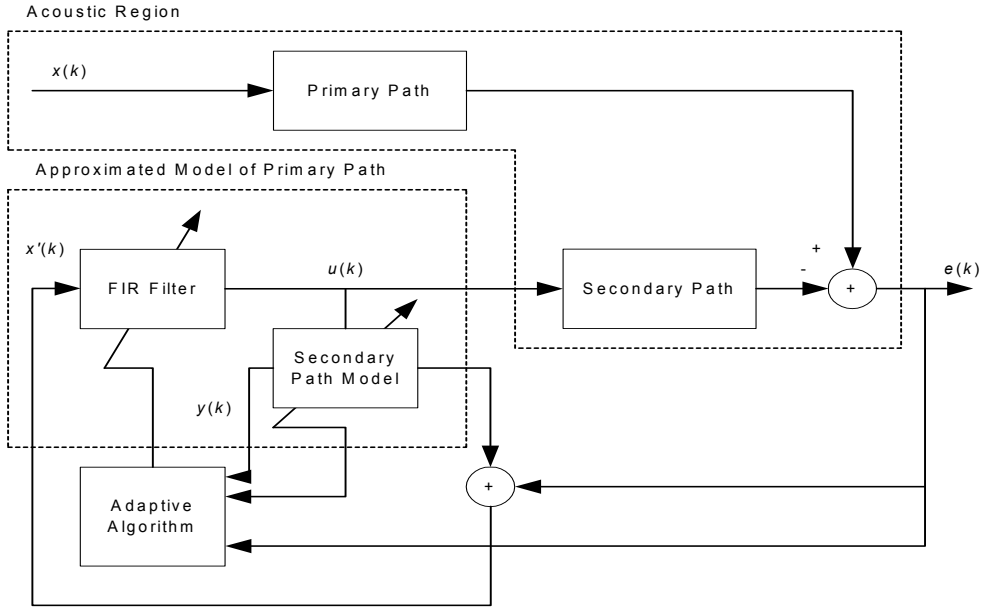

Figure 10 Feedback configuration.

Active noise cancellation using feedback configuration can be formulated by adopting the above algorithm, but now we employ adaptive predictor (see

Figure 10). Since reference microphone is not used, input signal to FIR filter is synthesized from

$$x'(k) = e(k) - y(k)$$

6 Experiment Setup and Results

Experiment setup of multichannel ANC inside an enclosure is shown in Figure 11. In this setup, two error sensors (microphones), two actuators (6“, 8 Ohm speakers), and one reference sensor are used. The objective of the ANC is to obtain quiet zones around each error microphone within a wooden 3-D enclosure, which mimics cabin of a vehicle. To implement active noise control computation and data acquisition, TMS320C6701 Evaluation Module DSP Board is used. The board is based on floating point TMS320C6701 DSP processor. The board is interfaced with computer host through PCI to enable real-time data exchange. Placement of actuators and sensors are shown in Figure 12.

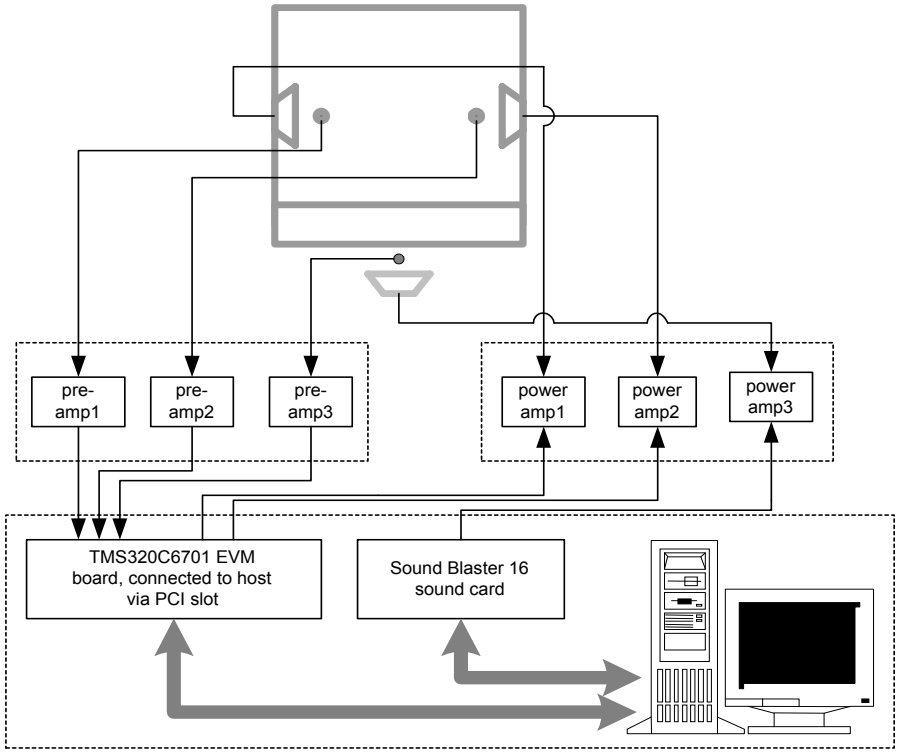

Figure 11 ANC Experiment setup.

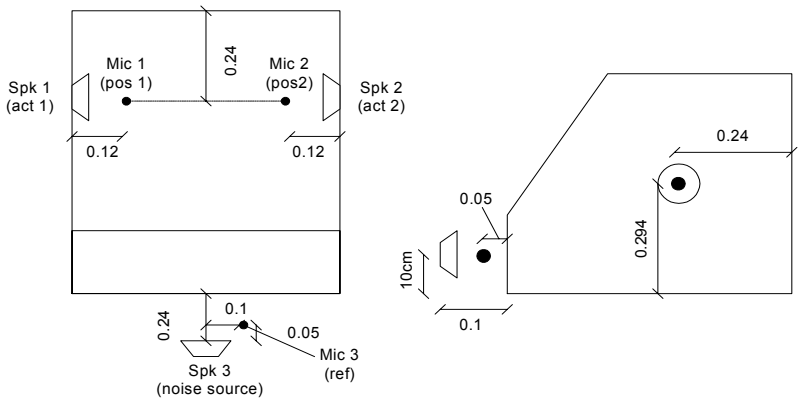

Figure 12 ANC Geometry (all distances are expressed in terms of λ).

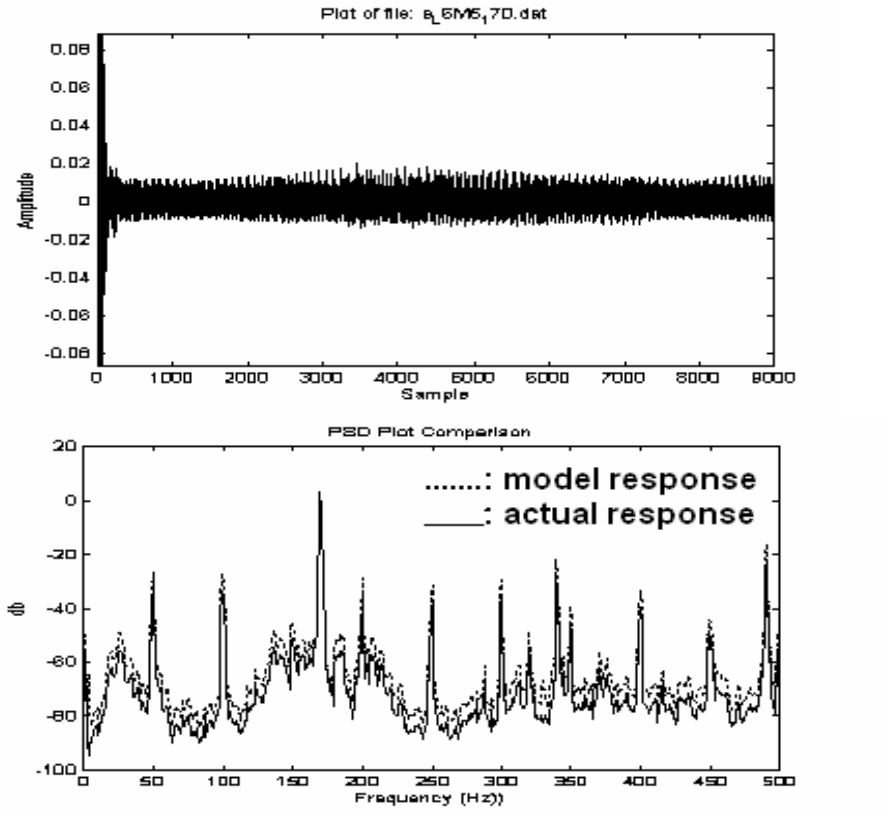

Figure 13 Experiment results of secondary path identification with noise freq. of 170Hz and 5^{th} order IIR filter, identification error with MSE= 2,8965e-5 (top), power spectral density (bottom).

Primary noise is generated through Sound Blaster 16 and controlled form within Windows operating system. The output of sound blaster, as well as of DSP, are applied to power amplifiers which in turn drive the speakers. Pre-amplifiers are used to amplify the signal measured by the microphones. Coding, debugging and real-time analysis are performed via Code Composer Studio.

Figure 13 shows experiment results of identification process of secondary path for single channel ANC using adaptive robust filter algorithm. We obtain quite small error with IIR filter which shows that model is accurate enough to represent behavior of secondary path. Shown at the bottom of Figure 13 is frequency response of IIR model and of actual secondary path. Note that in the frequency domain the model obtained approximates the frequency behavior of the secondary path.

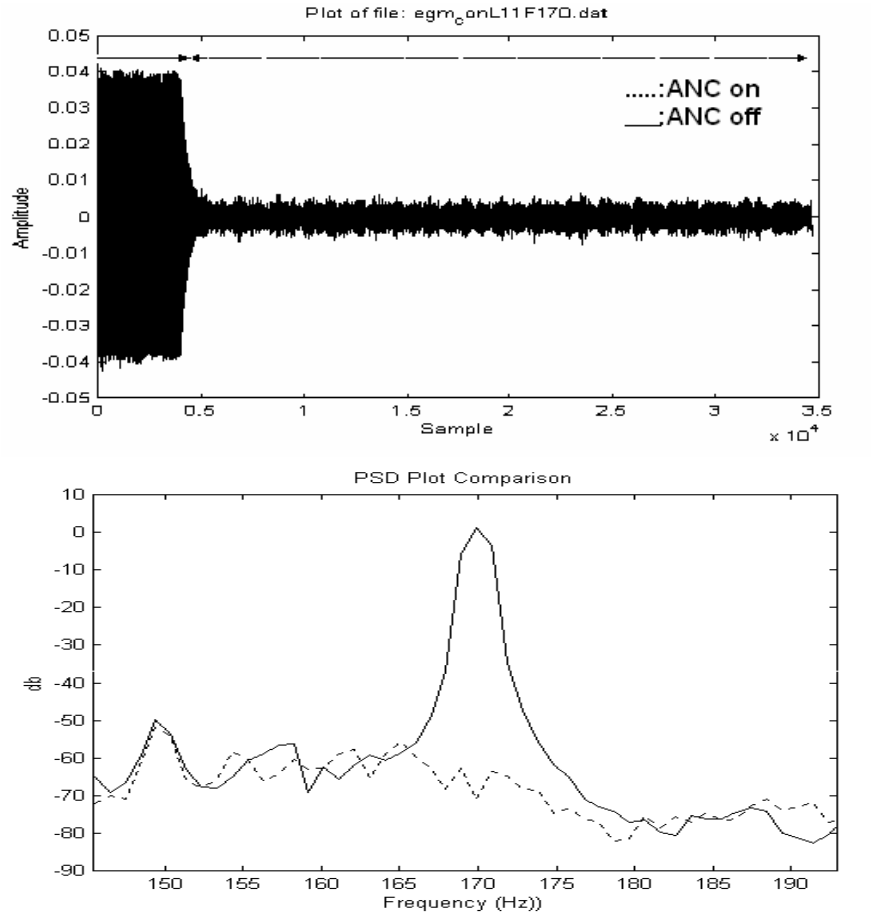

Figure 14 Experiment results of single channel ANC, noise residue (top) and power spectral density (bottom).

Figure 14 shows experiment results of single channel ANC using secondary path model obtained in previous experiment. Observe that transient response is fairly fast (1.5 second), while signal residue is sufficiently small. From power spectral density plot, attenuation at noise frequency (170Hz) reaches 74 dB.

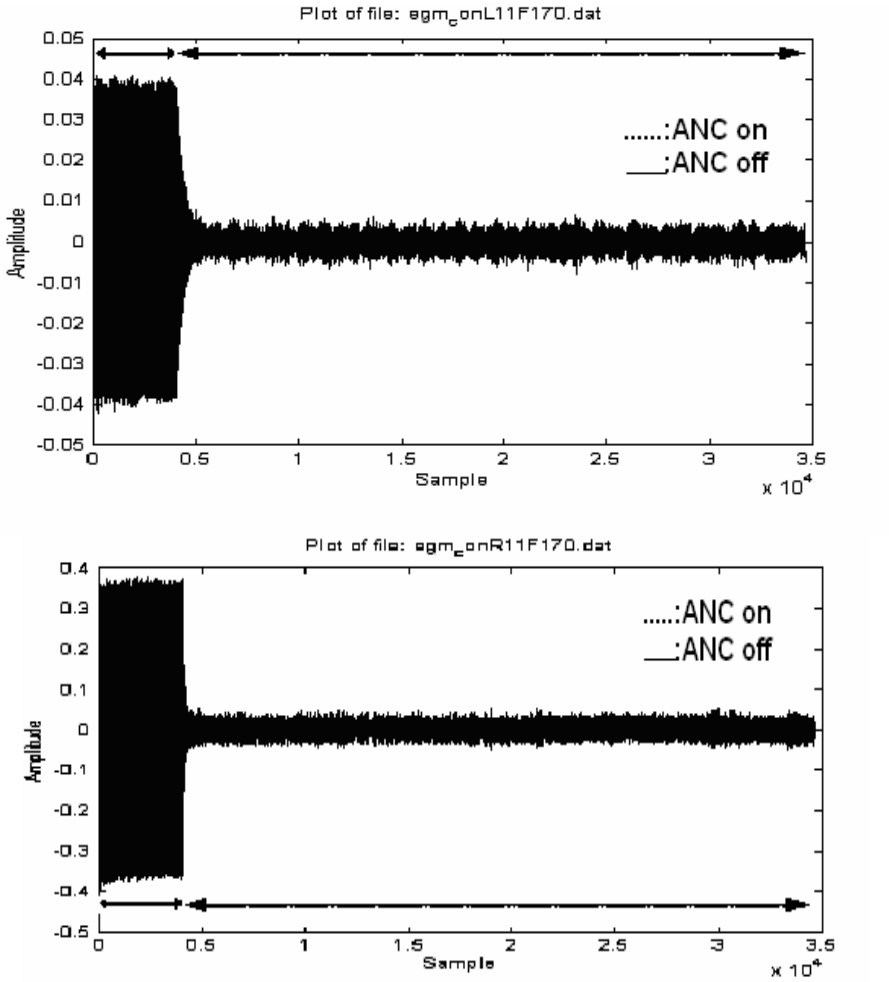

Figure 15 Comparison of FxLMS and Robust filter, FxLMS (top) and Robust filter (bottom).

Comparison of FxLMS and Robust filter algorithm is shown in Figure 15 (note the difference in scale). This comparison shows that attenuation level obtained by robust filter algorithm is better than that of FxLMS, without significantly degrading transient response. In fact, in most of the cases the transient responses for Robust filter are better than those of FxLMS.

Robustness property of H_∞ filter is examined in ANC experiment by shifting the position of error microphone 0.025λ from its original (nominal) position. The disturbance is applied for a period of time (5-10 seconds). The results are shown in Figure 16. Observe from this experiment that initially after microphone is shifted the amplitude of the noise residue increases but decreases afterwards.

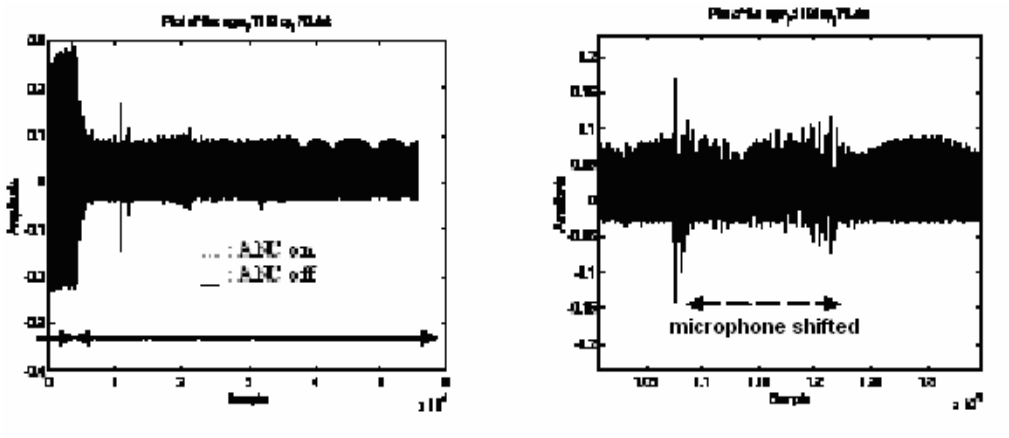

(a) (b)

Figure 16 Effect of disturbance by shifting the error microphone, (a) before disturbance is applied, and (b) effect of disturbance

Table 1 shows results of experiment with respect to the FIR filter order and to secondary path model order when the two types of uncertainty are applied. Note that robust filter achieves better noise attenuation level than that of FxLMS in case of tonal noise as well as superpositioned sinusoidal noise.

Noise frequency (Hz)	FIR order/ secondary model order	Type of uncertainty	Algorithm	Attenuation at noise main frequency(dB)	Transient (s)
170	11/1	Microphone shifting	Robust	48	0,4
170	3/4	Modeling/identification error	Robust	67	3
			FxLMS	42	4
170 and 210	11/4	Modeling/identification error	Robust	54 & 50	3
			FxLMS	28 & 25	3

Table 1 Results of single channel ANC with the uncertainty applied.

Experiment result for multichannel ANC is shown in Figure 17. In this experiment we use 1x2x2 configuration, that is, it employs 1 reference microphone, 2 speakers, and 2 error microphones. First, correlation between channels is omitted, i.e., a decentralized configuration is employed. In this experiment we obtain total (over all frequencies) noise attenuation level of 18.9144 dB at error microphone no. 1 and of 19.6670 dB at error microphone no. 2, while transient response is 0.1 second, which again shows the effectiveness of the H_∞ filter algorithm. The results are summarized in Table 2.

Experiment is also performed by considering correlation between channels, i.e., a centralized configuration is employed. Positions of noise sources are varied. The results are summarized in Table 3. Note that when the noise sources are spatially distributed, the total level of noise attenuation degrades substantially. However, at main frequency, only a slight degradation is observed.

Controller Order	Error Mic. Position	Noise Type	Total Reduction (dB)	Reduction at main Freq. (dB)	Transient Duration (seconds)
11	Microphone 1	Spatially centralized	18.9144	50	0.1
11	Microphone 2	Spatially centralized	19.6670	40	0.1

Table 2 Multichannel experiment results (correlation between channel is omitted).

Controller Order	Error Mic. Position	Noise Type	Total Reduction (dB)	Reduction at main Freq. (dB)	Transient Duration (seconds)
11	Microphone 1	Spatially centralized	18.4950	61	0.1
11	Microphone 2	Spatially centralized	19.7680	47	0.1
11	Microphone 1	Spatially distributed	8.0184	60	0.1
11	Microphone 2	Spatially distributed	14.4855	39	4

Table 3 Multichannel experiment results (correlation between channels is taken into account).

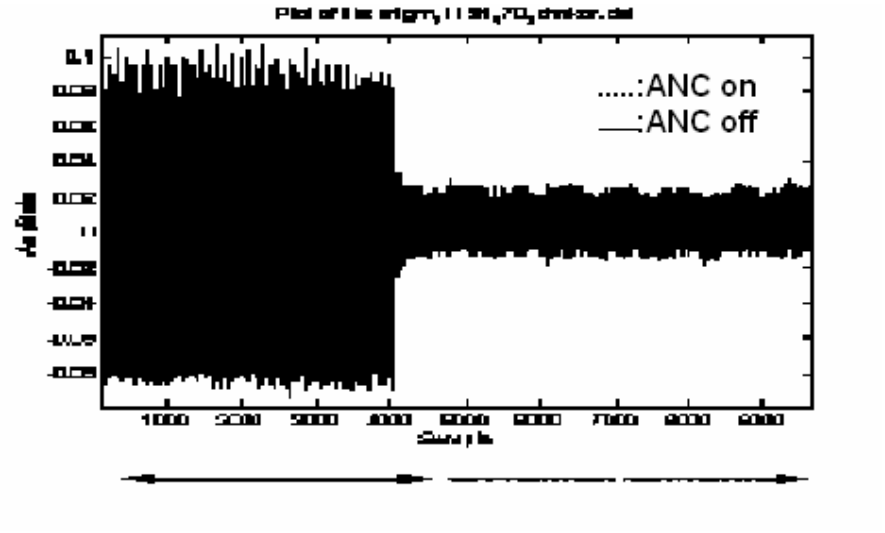

(a)

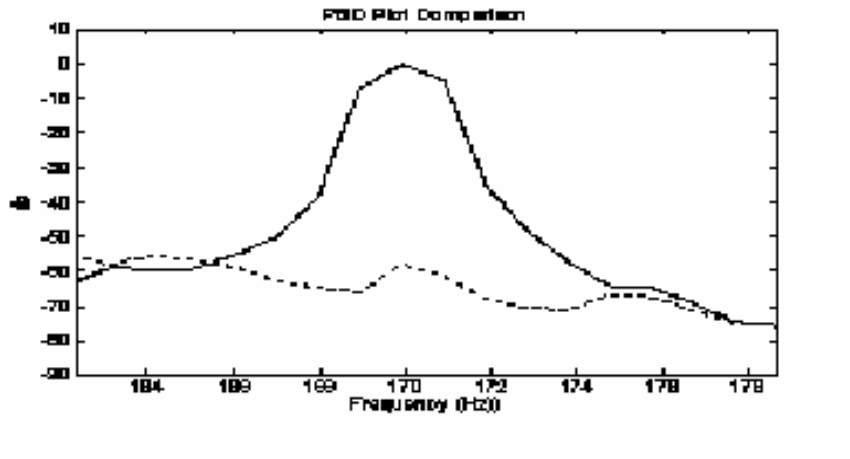

(b)

Figure 17 Experiment results of multichannel ANC with 1x2x2 configuration, a) Signal residue at one of the microphones and b) Power spectral density.

6 Conclusion

Active control using H_∞ method was shown to have better capability in attenuating low frequency noise within an 3-D enclosure as compared to conventional FxLMS algorithm. It was experimentally demonstrated that the system is robust with respect to modeling error due to inaccuracy in identification process, as well as to variations in microphone positions. Computational load of this algorithm is moderate, allowing real-time

implementation on DSP. Investigation on the distance of microphone shifting in which the ANC starts to fail and how it relates to the size of unstructured uncertainty predicted by the small gain theorem is left for future research. Extension of this work to nonlinear ANC using various nonlinear neural networks based filters can be found in [14-18].

References

1. Elliott, S. J. & Nelson, P. A., *Active Noise Control*, IEEE Signal Processing Magazine, vol. 10, no. 4, 12-35 (1993).
2. Elliott, S. J. & Boucher, C. C., *Interaction between Multiple Feedforward Active Control Systems*", IEEE Transactions on Speech and Audio Processing, vol. 2, no. 4, 521-530(1994).
3. Hassibi, B., Sayed, A. H., & T. Kailath, *Linear estimation in Krein spaces—Part II: Applications*, IEEE Trans. Automatic Control, vol. 41, no. 1 (1996).
4. Park, S. J., Yun, J. H., Park, Y. C. & Youn, D. H., *A Delayless Subband Active Noise Control System for Wideband Noise Control*, IEEE Trans. Speech and Audio Processing, vol. 9, no. 8 (2001).
5. Sayyarrodsari, B., How, J. P., Hassibi, B. & Carrier, A., *Estimation Based Synthesis of H_∞-Optimal Adaptive FIR Filters for Filtered-LMS Problems*, IEEE Trans. Signal Processing, vol. 49, no. 1 (2001).
6. Kuo, S. M., Kong, X. & Gan, W. S., *Applications of Adaptive Feedback Active Noise Control System*, IEEE Trans on Control System Technology, vol. 11, no. 2 (2003).
7. Kaiser, O., *Modeling and Robust Control of Active Noise Control Systems*, PhD Dissertation, Zwiss Federal Institute of Technology (1996).
8. Khargonekar, P. P. & Nagpal, K. M.," *Filtering and Smoothing in an H_∞-Seting*", IEEE Trans. Automat. Control, vol. 36, 151-166 (1991).
9. Kuo, Sen M. dan Morgan, D.R. *Active Noise Control Systems: Algorithms and DSP Implementations*, New York: John Wiley & Sons, Inc. (1996).
10. Sayyarrodsari, B., How, J. P., Hassibi, B. & Carrier, A., *An H_∞-Optimal Alternative to the FxLMS Algorithm*, Lokheed Martin Missiles & Space(1998).
11. Snyder, Scott D. & C.H. Hansen, "*Design considerations for active noise control systems implementing the multiple input, multiple output, multiple output LMS algorithm*," *J. Sound Vib.*, Vol. 141, pp. 409-424 (1990).
12. Widrow, B. & Stearns, S. D., *Adaptive Signal Processing*, Englewood Cliffs, NJ: Prentice Hall (1985).

13. Riyanto, B., *Decentralized Active Noise Control Using U-Filtered Algorithm: An Experimental Study*, Proc. International Conf. On Modeling, Identification and Control, Innsbruck, Austria (2000).
14. Riyanto, B., *On-Line Secondary Path Identification of Active Noise Control Using Neural Networks*, Proc. Int. Conf. Modeling and Simulation, Pittsburgh , USA (2000).
15. Riyanto, B. & Jayawardana, B., *Active Noise Control Using Recurrent Neural Networks*, Proc. Asian Control Conference, Singapore (2002).
16. Riyanto, B., *DSP Based Modeling and Control for Active Noise Cancellation Using Radial Basis Function Networks*, IEEE Symposium on Intelligent Control, Canada (2002).
17. Riyanto, B., *Active Noise Cancellation Using Recurrent Radial Basis Function Neural Networks*, Proc. IEEE Asia Pacific Conference on Circuits and Systems, Singapore (2002).
18. Riyanto, B., Uchida, K. & Jayawardana, B., *Active Noise Control in 3D Space Using Recurrent Neural Networks*, Proc. International Congress and Exposition on Noise Control Engineering, Korea (2003).
19. Riyanto, B. & Shimemura, E., *Reduced-Order Controllers for Discrete-Time Systems with Mixed H_2/H_∞ Performance Objectives,* Journal of Control and Computers, Vol. 20, 84-88, no.3 (1992).
20. Riyanto, B., Shimemura, E. & Uchida, K., *Mixed H_2/H_∞ Control with Root Clustering,* Trans. of Society of Instrumentation and Control Engineer, vol. 29, no. 3, 263-271 (1993).
21. Riyanto, B., Shimemura, E. & Uchida, K., *Variance Constrained H_2/H_∞ Control,* International Journal of Systems Science, vol. 24, no. 11, 1197-2017 (1992).
22. Riyanto, B., Shimemura, E. & Uchida, K., *Mixed H_2/H_∞ Control with Pole Placement in a Class of Regions,* Journal of Optimal Control Applications and Methods, John Wiley & Sons (1994).
23. Riyanto, B. & Sastrokusumo, U., *H_∞ Filter for Discrete-Time Systems and Its Comparison to Classical Kalman Filter,* Proc. International Conf. Telecommunication, (1995).
24. Doyle, J. C., Glover, K., Khargonekar, P. & Francis, B., *State Space Solution to Standard H_2 and H_∞ Control Problems,* IEEE Trans. Automatic Control, vol. 34, no. 8 (1989).